Heat wave hinders green wave: The impact of climate extreme on the phenology of a mountain grassland

Contents lists available at ScienceDirect

Agricultural and Forest Meteorology

journal homepage: www.elsevier.com

Heat wave hinders green wave: The impact of climate extreme on the phenology of a mountain grassland

Edoardo Cremonese[a,*], Gianluca Filippa[a], Marta Galvagno[a], Consolata Siniscalco[b], Ludovica Oddi[b], Umberto Morra di Cella[a], Mirco Migliavacca[c]

[a] Environmental Protection Agency of Aosta Valley, Climate Change Unit, Italy
[b] Department of Life Sciences and Systems Biology, University of Torino, Italy
[c] Department Biogeochemical Integration, Max Planck Institute for Biogeochemistry, Jena, Germany

ARTICLE INFO

Keywords:
Climate extremes
Mountain grassland
Heat wave
Drought
Phenology
Phenocam

ABSTRACT

Climate extremes can have tremendous impacts on the terrestrial biosphere and their frequency is very likely going to increase in the coming years. In this study we examine the impact of the 2015 summer heat wave on a mountain grassland in the Western European Alps by jointly analyzing phenocam greenness (GCC) trajectories, proximal sensing, CO_2 flux data and structural canopy traits. Phenocam effectively tracked the impact of the heat wave, showing 39% of reduction in maximum canopy greenness and a senescence advance of 32 days compared to mean values. The same patterns (*i.e.* reduction of maximum values and senescence advance) were observed for all considered canopy traits and photosynthetic ecosystem functional properties, in particular the maximum light-saturated rate of CO_2 uptake (A_{max}), LAI and PRI. Pixel-level analysis of phenocam images allowed us to further highlight that forbs were more heavily impacted than grasses. Moreover the effect of the extreme event on greenness seasonal course was evaluated testing new formulations of the Growing Season Index (GSI) model. Results demonstrate that a combination of water and high temperature stress was responsible for the observed reduction of canopy greenness during the heat wave.

1. Introduction

Global warming is occurring fast in the European Alps (Beniston, 2012) and an increase of climate extremes is likely going to occur in this region (Gobiet et al., 2013; IPCC, 2013) hosting some of the most ecologically sensitive ecosystems of the planet (Seddon et al., 2016). Climate extremes are known to have exceptional impacts on the terrestrial biosphere that can result in ecosystem productivity reduction (Reichstein et al., 2013; Bahn et al., 2014; Frank et al., 2015; Rammig et al., 2015), altered ecological dynamics, community composition modification and biodiversity losses (Smith, 2011; Jung et al., 2014; Fuchslueger et al., 2014).

Phenology is one of the most effective biological indicators of climate change impacts on the terrestrial biosphere (Scheffers et al., 2016). Many studies highlighted the relationship between climate change and phenology (*e.g.* Buitenwerf et al., 2015; Richardson et al., 2013), as well as the impact that climate extremes can have on spring events such as flowering and foliar development or senescence (Reyer et al., 2013; Menzel et al., 2015; Hufkens et al., 2012a).

By providing continuous sub-daily images of canopy development, phenocams (*i.e.* repeat digital photography) are useful tools for phenology monitoring (Richardson et al., 2009) leading to an increase in phenocam deployment in the last years worldwide (Brown et al., 2016; Wingate et al., 2015; Nasahara and Nagai, 2015). Indeed, greenness index (Richardson et al., 2007) derived from phenocam imagery is used to track the green wave (*i.e.* the seasonal greening phenology, Schwartz, 1998) of many terrestrial ecosystems such as forests (Sonnentag et al., 2012; Hufkens et al., 2012a; Nagai et al., 2011), grasslands (Migliavacca et al., 2011; Hufkens et al., 2016; Inoue et al., 2015), peatlands (Peichl et al., 2013) and crops (Sakamoto et al., 2012; Wingate et al., 2015). Other authors analyzed the relationship between greenness index and ecosystem productivity (Toomey et al., 2015; Saitoh et al., 2012; Mizunuma et al., 2013; Knox et al., 2017), canopy functional and structural properties (Keenan et al., 2014; Yang

* Corresponding author.
Email address: e.cremonese@arpa.vda.it (E. Cremonese)

https://doi.org/10.1016/j.agrformet.2017.08.016
Received 11 May 2017; Received in revised form 11 August 2017; Accepted 14 August 2017
Available online xxx

et al., 2014) and disturbance events (Nagler et al., 2014; Zhou et al., 2017). Recently Menzel et al. (2015) and Hufkens et al. (2012b) demonstrated that phenocams can also be used to infer the impact of climate extremes on spring canopy development. Phenocam analysis is generally based on the extraction of canopy greenness information from specific regions of interest of the scene. In the last years, pixel-level analysis of phenocam imagery has been proposed as a new very promising approach to infer the spatial distribution of phenologically different individuals or species within the canopy and their differential response to climate cues (Julitta et al., 2014; Filippa et al., 2016; Snyder et al., 2016). Moreover, Migliavacca et al. (2011) demonstrated that phenocam canopy greenness can also be used to constrain phenological models such as the Growing Season Index model (GSI, Jolly et al., 2005) for the simulation of canopy development and for the identification of the main meteorological factors controlling plant phenology. Indeed the GSI model offers opportunities to disentangle the influence that meteorological drivers can have on canopy greenness during climate anomalies.

The relationship between the phenology of tree species and climate drivers has been thoroughly investigated by means of long-term data (*e.g.* Menzel et al., 2006; Fu et al., 2015; Zohner et al., 2016), while less studies focused on alpine grassland phenology (*e.g.* Vitasse et al., 2016; CaraDonna and Inouye, 2015; Filippa et al., 2015; Wipf and Rixen, 2010). Mountain grasslands are ecosystems vulnerable to climate extremes like early or delayed snowmelt, heat waves and droughts (De Boeck et al., 2015; Galvagno et al., 2013; Choler, 2015). The impacts of these extremes mainly depend on their intensity and timing (Sippel et al., 2016), ecosystem species composition and diversity and the interaction of biotic and abiotic factors (Hoover et al., 2014; Kreyling et al., 2011; Vogel et al., 2012; Ernakovich et al., 2014).

In 2015 heat records were broken worldwide (Heffernan, 2016; Tollefson, 2015) and in particular in July 2015, Europe experienced extremely hot temperatures and low precipitations (World Meteorological Organization, 2016). In this study we take advantage of this event to evaluate the impact of a climate extreme on the phenology of a mountain grassland in the Western European Alps using phenocam data. The main objectives of the study are: (i) to analyze heat wave impact on canopy green wave and relate it to other functional and structural canopy traits, (ii) to evaluate the occurrence of differential effects on plant functional types using pixel-level analysis and (iii) to disentangle the role of meteorological drivers on greenness during the heat wave.

2. Materials and methods

2.1. Study site

The study is conducted in an abandoned subalpine grassland (Torgnon, Italy, Galvagno et al., 2013) in the Western European Alps located at 2160 m asl (45°50′40″ N, 7°34′41″ E). Dominant vegetation mainly consists of grasses, (*Nardus stricta*) with co-dominant forbs species like *Arnica montana*, *Trifolium alpinum* and *Geum montanum*. The site is characterized by a mean annual temperature of 3.1 °C and mean annual precipitation of about 880 mm. A thick snow mantle generally covers the site from the end of October to late May limiting the growing season length to an average of five months. The peak value of Leaf Area Index (LAI) is on average 2.2 m^2 m^2 and maximum canopy height is 20 cm. The site is characterized by undulating terrain with a heterogeneous microtopography (< 50 cm); following snowmelt spatial patterns, forbs species tend to be located in concave areas, while grasses occupy convex areas (Pintaldi et al., 2016).

2.2. Data collection and processing

2.2.1. Phenocam and meteorological data

Phenocam images are collected using a Nikon D5000 digital camera controlled by a raspberry-Pi computer. Following Richardson et al. (2007), the camera is installed 2.5 m above the ground, pointing north and set at an angle of about 20° below horizontal. Images, collected hourly from 10.00 to 16.00 with exposure mode and white balance set respectively to automatic and fixed, are saved in JPEG format at a resolution of 1024 × 2048 pixels. The present study is based on images covering the period 2013–2015. Canopy greenness (green chromatic coordinate, GCC, Richardson et al., 2007), is computed following Eq. (1) for a selected region of interest (ROI) located in the foreground portion of the images.

$$\mathrm{GCC} = \frac{G_{\mathrm{DN}}}{R_{\mathrm{DN}} + G_{\mathrm{DN}} + B_{\mathrm{DN}}} \quad (1)$$

where R_{DN}, G_{DN} and B_{DN} are the red, green and blue digital numbers (DN) of each color channel in JPEG images, respectively. Daily filtered GCC time series are obtained using the phenopix R package (Filippa et al., 2016), following the filtering approach suggested by Sonnentag et al. (2012). The entire phenocam dataset of the site is available at https://phenocam.sr.unh.edu/webcam/sites/torgnon-nd/. Since 2008, a weather station provides 30-min averaged records of air temperature (HMP45, Vaisala), photosynthetically active radiation (LI-190, LI-COR), precipitation (OTT Pluvio2, OTT Hydromet) and soil water content (CS-616, Campbell Scientific).

2.2.2. Gross primary productivity and photosynthetic ecosystem functional properties

Eddy covariance measures of CO_2 fluxes are carried out continuously since 2008. Details on instrumental setup, measurements and data processing are provided in Galvagno et al. (2013, 2017). Estimates of gross primary productivity (GPP) are obtained following Reichstein et al. (2005) and Lasslop et al. (2010) approaches implemented in the online tool available at http://www.bgc-jena.mpg.de/~MDIwork/eddyproc/index.php. Ecosystem functional properties related to photosynthesis (Reichstein et al., 2014) are estimated using the light-response curve of photosynthesis (Eq. (2)) describing the relationship between Net Ecosystem Exchange (NEE) and photosynthetically active radiation (PAR). The rectangular hyperbolic light-response function (Falge et al., 2001) is used:

$$\mathrm{NEE} = \frac{A_{\max}\alpha\mathrm{PAR}}{\alpha\mathrm{PAR} + A_{\max}} + R_{\mathrm{eco}} \quad (2)$$

where A_{max} (μmol CO_2 m^{-2} s^{-1}) is the maximum light-saturated rate of CO_2 uptake, α (μmol CO_2 $\mu mol^{-1}_{photons}$) is the canopy light use efficiency representing the initial slope of the light-response curve, and R_{eco} (μmol CO_2 m^{-2} s^{-1}) is the ecosystem respiration. Model parameters are estimated by fitting Eq. (2) to non gap-filled, daytime half-hourly NEE data with a 15-day moving window shifted each 5 days and assigned to the central day of the moving window. Daily midday averages (average of all data from 11.00 to 13.00 LST) of GPP and daily A_{max} and α values are used for further analysis.

2.2.3. Spectral vegetation indexes

Canopy spectral properties are measured with SKR1800 sensors (Skye Instruments) collecting spectral signatures of the canopy every 5 min. Spectral data are used to compute vegetation indices (VIs) related to canopy structure such as the Normalized Difference Vegetation Index (NDVI, Rouse et al., 1974, Eq. (3)) and to canopy functioning

such as the Photochemical Reflectance Index (PRI, Gamon et al., 1997, Eq. (4))

$$\mathrm{NDVI} = \frac{\rho_{860} - \rho_{640}}{\rho_{860} + \rho_{640}} \tag{3}$$

$$\mathrm{PRI} = \frac{\rho_{531} - \rho_{570}}{\rho_{531} + \rho_{570}} \tag{4}$$

where ρ_x is the reflectance computed at the x wavelength in nm. The fraction of the photosynthetically active radiation absorbed by the canopy (F_{apar}) is calculated using incident, reflected and below canopy PAR measures following Eklundh et al. (2011) and Olofsson and Eklundh (2007). For consistency, daily midday averages of VIs and F_{apar} are used for further analyses.

2.2.4. LAI and biomass

Leaf Area Index (LAI), green and dry aboveground biomass are measured every 10–15 days during the growing season, by clipping a 30 × 30 cm vegetation quadrat to 2 mm above the ground at 12 selected plots in the study area. After harvesting, the material is separated in green and dry mass, dried to constant weight at 60 °C for 48 h and weighed. LAI is determined on the same material using an area meter (model LI-3100, LI-COR). For details see Filippa et al. (2015). LAI and the ratio of green to total aboveground biomass (GT_{biom}) are used in this study.

2.3. Heat wave impact metrics

The time series of all collected variables (*i.e. GCC*, *GPP*, A_{max}, α, *VIs*, *LAI* and GT_{biom}) describe the phenology of functional and structural canopy traits at the study site. In order to capture the seasonal trajectory of these variables, all time series are fitted with a double logistic function following the formulation proposed by Klosterman et al. (2014) using the phenopix R package (Filippa et al., 2016).

Since the heat wave occurred from late June throughout July, the analysis of its impact is mainly focused on the first part of the seasonal trajectory of each variable. In particular two heat wave impact metrics are used: (i) peak value reduction (PR [%], *i.e.* the difference between peak value in 2015 and the average peak values in 2013–2014) and (ii) peak advance (PA [days], *i.e.* the difference between 2015 peak date and the average 2013–2014 date). PR and PA uncertainties are estimated recursively fitting randomly-noised original data and extracting the considered phenophases from fitted curves ensemble as proposed in Filippa et al. (2016). Impact metrics and their uncertainties are calculated to evaluate the consistency of heat wave effect on all considered canopy traits. Secondly, in order to group canopy traits according to their response to the heat wave, the partitioning around medoids (PAM) cluster analysis is applied using the cluster R package (Maechler et al., 2016). The optimal number of clusters is defined by evaluating the reduction of the total within-groups sum of squares (Kaufman and Rousseeuw, 1987; Reynolds et al., 2006).

2.4. Impact on plant functional types

A pixel-level analysis of phenocam images (Filippa et al., 2016) is conducted to evaluate the occurrence of differences in heat wave impact between the two predominant plant functional types of the site namely grasses and forbs. The phenology of these two types mainly differs in the first spring phases (Julitta et al., 2014): forbs, represented by more opportunistic species (*e.g. A. montana*, *G. montanum*, *Potentilla aurea*, etc.), have an earlier start of growth compared to *N. stricta*, that is the dominant grass species.

The seasonal GCC trajectory of each pixel in the ROI is fitted using the double logistic formulation of Klosterman et al. (2014) and the start of the growing season for each pixel is then estimated from the fitted curve following Gu et al. (2009) approach. Grasses and forbs pixels are separated with a *K*-means cluster analysis on the start of season date for the 2013–2015 period. Clustering results are validated with field vegetation survey as in Julitta et al. (2014). Once forbs and grasses pixels are separated, heat wave impact metrics are computed for each pixel. For this analysis a third impact metric is used: the reduction of the area under the normalized GCC curve (AUC). The difference between AUC in 2015 and mean AUC is used as an estimate of the greenness reduction due to the heat wave. The significance of the differences in the three heat wave impact metrics (PR, PA and AUC) between the two plant functional types is tested with the analysis of variance.

2.5. GSI modeling

The Growing Season Index model (GSI) is used in combination with GCC time series to disentangle the influence of meteorological drivers on canopy greenness during the heat wave. GSI was originally developed by Jolly et al. (2005) to model canopy development using three climatic limiting factors: minimum daily temperature, T_{min} (°C), photoperiod, Ph (h) and mean day-light vapor pressure deficit, VPD (hPa). The daily value of GSI is computed as the 21-day running average of the index iGSI calculated as the product of the limiting factors. Limiting factors can vary between 0 and 1 following step functions and represent maximum and minimum ranges above/below which canopy development is fully constrained or unconstrained, respectively. Migliavacca et al. (2011) demonstrated that the simulation of canopy development at the study site can be improved by including limiting factors that are more relevant for mountain grasslands such as snow cover and soil water content (SWC). In this study a further modification of the GSI model is proposed to test if the inclusion of a temperature optimum function ($f(T_{opt})$), formulated as in Eq. (5), can result in a better representation of canopy development constraints driven by both low and high temperature limitations.

$$f(T_{\mathrm{opt}}) = \frac{(T - T_{\max})(T - T_{\min})}{((T - T_{\max})(T - T_{\min})) - (T - T_{\mathrm{opt}})^2} \tag{5}$$

where T is the mean daily temperature, T_{max} and T_{min} define the temperature range and T_{opt} is T value of optimal canopy development.

Four model formulations are tested (Table 1). All model formulations include the fundamental control on phenology of snow and photoperiod ($f(Snow)$ and $f(Ph)$) observed in previous studies (Migliavacca et al., 2011; Galvagno et al., 2013; Julitta et al., 2014) and include two formulations for the temperature control (step function, $f(T_{min})$(Migliavacca et al., 2011) and optimum function, $f(T_{opt})$ (Eq. (5))) and for the water control ($f(VPD)$ and $f(SWC)$, Migliavacca et al., 2011).

An optimization approach is followed to find the model formulation that can better reproduce observed canopy greenness in the period 2013–2015. For each formulation (Table 1), model parameters are estimated using a combination of a global optimization algorithm, Markov Chain Monte Carlo (MCMC), and a local optimization algorithm based on a quasi-newton approach. In the first step we use a MCMC algorithm with a delayed rejection and adaptive Metropolis procedure (Haario et al., 2006). As prior a uniform distribution is used. The likelihood function is the sum of squared error between observed GCC rescaled between 0 and 1 and modeled GSI. The algorithm used is implemented in the FME package in R (R Core Team, 2015). In a second step, we use a quasi-Newton algorithm implemented in the op-

Table 1
GSI model formulations tested in this study. Gray cells indicate the limiting factors included in each formulation: $f(T_{min})$, minimum temperature; $f(T_{opt})$, optimum temperature (Eq. (5)); $f(Ph)$, photoperiod; $f(Snow)$, snow; $f(VPD)$, mean day-light vapor pressure deficit and $f(SWC)$, soil water content.

		$f(T_{min})$	$f(T_{opt})$	$f(Ph)$	$f(Snow)$	$f(VPD)$	$f(SWC)$
Migliavacca et al. (2011)	GSI_{Snow}						
This study	$GSI_{SWC+Snow}$						
This study	$GSI_{T_{opt}+Snow}$						
This study	$GSI_{T_{opt}+SWC+Snow}$						

tim() R function using as first guess the results of the MCMC optimization. The residual sum of squares between observed and modeled data (RSS) is used as cost function in this second step. The main fitting statistics (r^2, the root mean square error, RMSE, and the modeling efficiency, EF) between observed and modeled data are computed to evaluate the overall accuracy of fitted models (Janssen and Heuberger, 1995). To identify the best model formulation, we compute the corrected Akaike Information Criterion (AICc, Akaike, 1992) as in Migliavacca et al. (2012), that is a useful indicator accounting for the trade-off between model complexity (*i.e.* number of parameters) and accuracy (*i.e.* performances of statistics). The lower is the AICc the better is the model, considering also its complexity.

3. Results

3.1. Climate data

Fig. 1 shows the deviation of 2015 growing season air temperature, precipitation and SWC from 2008–2014 mean values at the study site. A warm and dry spell occurred in the first 10 days of June followed by a normal period. From the end of June and throughout July, the ecosystem was hit by a second long period of hot temperature and precipitation absence that caused a progressive drying of the soil. SWC values started to decrease around the 20th of June and reached a minimum plateau lasting more than 20 days until the first days of August. These data confirm that during the heat wave, the ecosystem experienced a prolonged and intense co-occurrence of hot temperature and drought.

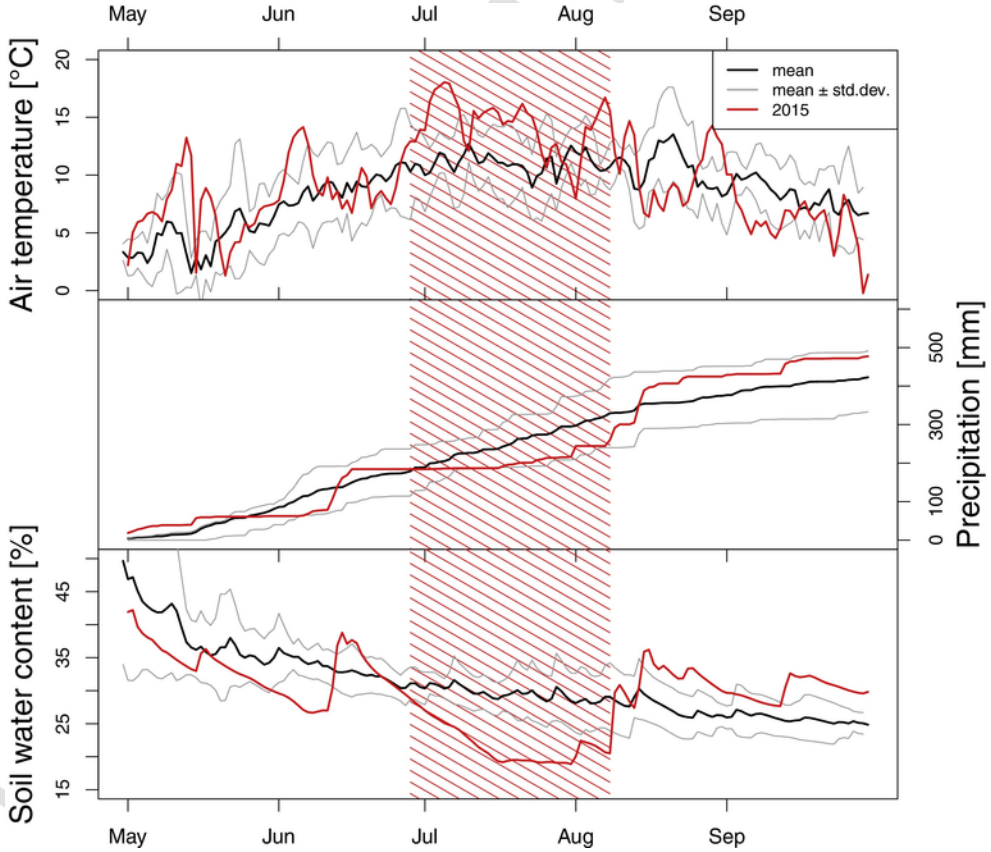

Fig. 1. 2015 (May–September) daily air temperature, precipitation and soil water content compared to 2008–2014 averages at the study site. Red lines represent 2015 values; black and gray curves indicate 2008–2014 mean and 2008–2014 mean ± standard deviation, respectively. The red shaded area indicates the heat wave duration. (For interpretation of the references to color in this figure legend, the reader is referred to the web version of the article.)

3.2. Canopy response to heat wave

The seasonal trajectory of canopy greenness is shown in Fig. 2. In 2015, the upturn date (*i.e.* start of spring growth) occurred approximately three weeks (DOY 143 ± 2) after snow melt (DOY 119). Compared to previous years (2013–2014), start of growth in 2015 is slightly earlier (4 and 16 days respectively) as a result of an earlier snow melt. Around the 20th of June (DOY 174 ± 0.7), thus at the begin of the second warm period, GCC peaked and started a long yellowing phase. Compared to previous years, a much lower maximum canopy greenness is reached in 2015 followed by an early start of senescence; in particular GCC shows a PR of 39.6 ± 1.03% and PA of 32 ± 0.75 days.

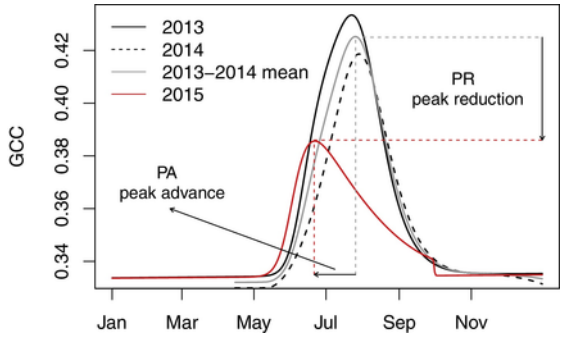

Fig. 2. Fitted time series of GCC of the three years considered in the present study. The continuous gray line indicates 2013–2014 mean that is used as a reference to compute heat wave impact metrics. Horizontal and vertical dashed lines, indicating peak values and peak dates in 2015 (red) and 2013–2014 mean (gray), are reported to illustrate how heat wave impact metrics (*i.e.* PR and PA) are computed. (For interpretation of the references to color in this figure legend, the reader is referred to the web version of the article.)

We examined the effect of the heat wave on all measured canopy traits and we found a common response, that is a reduction of maximum values and an early senescence. Indeed PR values range between 2.1 and 39.6% and PA values range between 4 and 43 days for all considered canopy traits (Fig. 3).

Some traits show impact metrics similar to what was observed for GCC, while others indicate a less intense impact. In particular, the cluster analysis (Fig. 4) highlights the presence of three groups: one including heavily impacted parameters (*GCC*, *PRI*, A_{max} and *LAI*), a second intermediate group (α, GT_{biom}) and the third one including less severely affected parameters (*GPP*, *NDVI* and F_{apar}).

3.3. Plant functional types

Forbs and grasses GCC seasonal course in 2015 compared to 2013–2014 mean and heat wave impact metrics (PR, PA and AUC) of the two plant functional types are reported in Fig. 5. PR values of grasses (42 ± 0.6%) and forbs (41 ± 1.0%) pixels are not statistically different ($p = 0.25$), indicating that both functional types experienced a similar reduction of maximum greenness. Conversely, forbs show a significantly higher PA (33 ± 0.6 and 30 ± 0.4 days for forbs and grasses respectively, $p < 0.001$) indicating that senescence advance for forbs was greater than for grasses. At the same time forbs experienced a stronger AUC reduction (31 ± 0.8% and 28 ± 0.6% for forbs and grasses respectively, $p = 0.008$), suggesting an overall lower impact on the seasonal course of GCC for grasses. In summary, the pixel-level analysis shows that two out of the three considered heat wave impact metrics indicate forbs as the functional type most affected by the heat wave.

3.4. GSI model results

The GSI model formulation that results in the most accurate simulation of greenness seasonal course is $GSI_{Topt+SWC+Snow}$. This formulation includes low and high temperature (T_{opt}), soil water content (SWC),

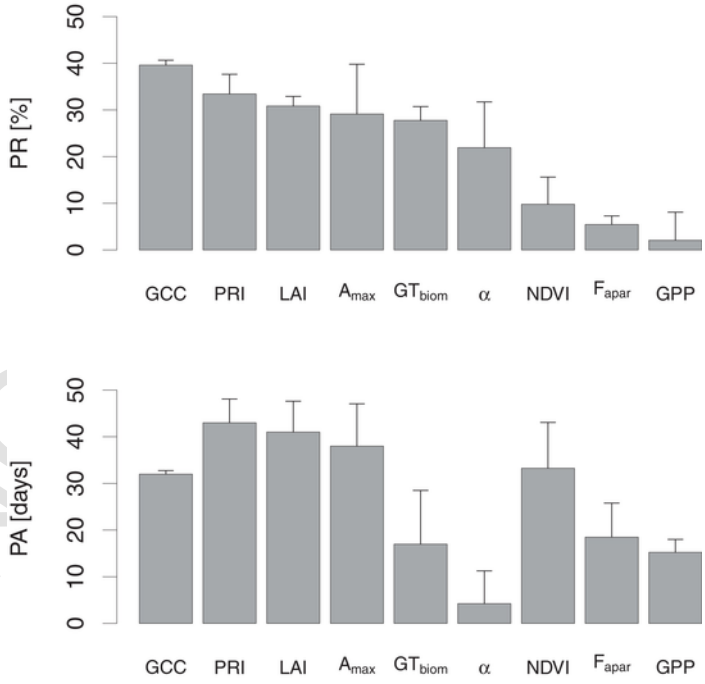

Fig. 3. Canopy traits heat wave impact metrics: peak value reduction (PR [%], upper panel) indicates the difference between 2015 and mean peak value; peak date advance (PA [days], lower panel) indicates the difference between 2015 and the mean peak date. Error bars represent the 0.1–0.9 quantile range of PR and PA values distribution.

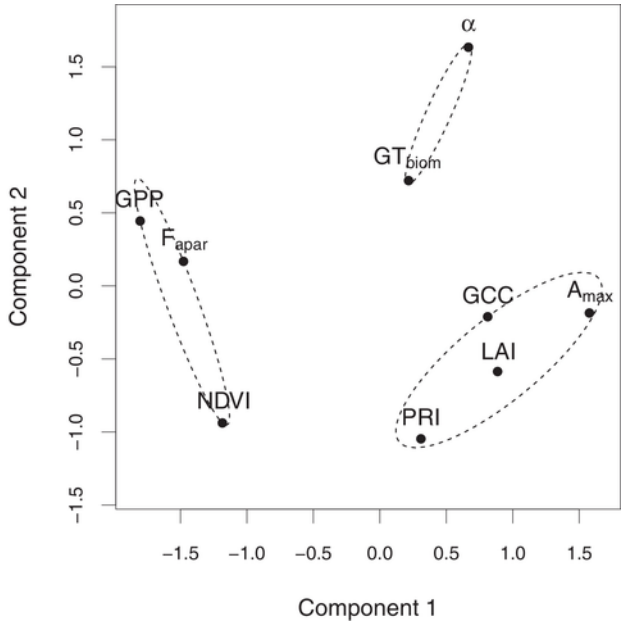

Fig. 4. Cluster analysis grouping canopy greenness, canopy traits and photosynthetic ecosystem functional properties according to their response to the heat wave.

photoperiod and snow limitation effects. Table 2 in particular shows that $GSI_{Topt+SWC+Snow}$ is the formulation with the lowest RMSE (0.118), the highest EF (0.801) and, despite having a higher model complexity, the lowest AICc. Table 2 also shows that all formulations including T_{opt} give better results when compared to formulations previously tested in this ecosystem (GSI_{Snow} and $GSI_{SWC+Snow}$, Migliavacca et al., 2011), which included only low temperature constraining effect (T_{min}). This result highlights that also high temperature plays an important role in constraining the seasonal course of greenness during warm years in this mountain grassland. Furthermore, $GSI_{Topt+SWC+Snow}$ gives better results than $GSI_{Topt+Snow}$ indicating that water limitation effects are better described by model formulation using soil water content instead of VPD.

4. Discussion

This study evaluates the impact of 2015 summer heat wave on a mountain grassland, by integrating the analysis of phenocam images, functional and structural canopy traits, photosynthetic ecosystem functional properties and phenological modeling.

The analysis of long term climate data, collected at a distance of ~ 30 km by a meteorological station belonging to the regional weather service, shows that July 2015 had an air temperature anomaly of +4.3 °C and was the hottest July in the period 1974–2015; 2015 anomaly is greater than what was observed in 2003 during the well known heat wave that had dramatic impacts on ecosystems and human society in central Europe (García-Herrera et al., 2010; Ciais et al., 2005). Considering precipitation, July 2015 corresponds to the 5th percentile of long term precipitation distribution, highlighting the co-occurrence of extremely hot and dry conditions. The exceptionally long period of hot temperature and progressive soil drying, occurring from the end of June to the end of July (Fig. 1), interrupted canopy greening and led to a long lasting yellowing phase. The heat wave hindered the seasonal green wave causing a reduction of yearly maximum greenness of about 40% and the onset of senescence occurring one month earlier than previous years. After the climate anomaly, the month of August was characterized by air temperature (11.14 ± 4.1 °C) close to average values (11.16 ± 3.8 °C, August 2008–2014) and very high monthly precipitation sums (218 mm vs. 88 ± 34 mm, August 2015 sum vs. August 2008–2014 mean ± sd sum) which completely rewetted the soil (Fig. 1). Previous studies demonstrated that canopy re-greening can occur after rain pulses in grasslands (*e.g.* Zelikova et al., 2015; Zhou et al., 2017) and this process was even observed at the study site in 2009 (Migliavacca et al., 2011). However, despite the favorable conditions observed in August 2015, canopy senescence continued and re-greening was not detected. This suggests that the intensity and the duration of

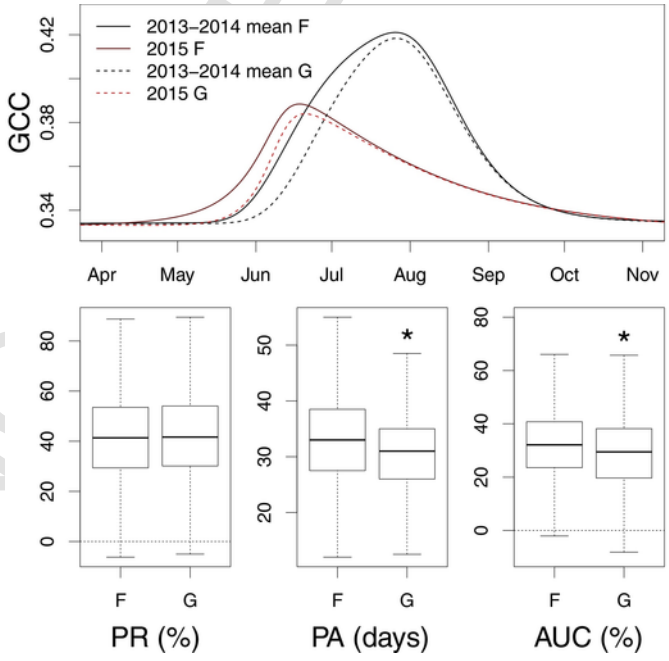

Fig. 5. (Upper panel) 2015 mean GCC time series of forbs (F) and grasses (G) pixels (continuous and dashed red lines respectively) compared to 2013–2014 mean (continuous and dashed black lines respectively). (Lower panel) Boxplots of peak reduction (PR, left) peak advance (PA, center) and seasonal greenness reduction (AUC, right) of forbs (F) and grasses (G). Asterisks denote significant differences between the means (Anova test, $p < 0.05$). (For interpretation of the references to color in this figure legend, the reader is referred to the web version of the article.)

Table 2
Fitting statistics of the different formulations of GSI model (Table 1). r^2 is the coefficient of determination, RMSE is the root mean square error, EF is the modeling efficiency, AICc is the corrected Akaike Information Criterion.

	r^2	RMSE	EF	AICc
GSI_{Snow}	0.763	0.130	0.724	−36.500
$GSI_{SWC+Snow}$	0.767	0.129	0.742	−36.546
$GSI_{Topt+Snow}$	0.800	0.120	0.785	−43.664
$GSI_{Topt+SWC+Snow}$	0.809	0.118	0.801	−43.865

June–July heat wave likely pushed the ecosystem toward a tipping point (Kreyling et al., 2014; Reichstein et al., 2013) that triggered a profound and irreversible senescing phase hampering any recovery (*i.e.* re-greening) during the favorable August conditions. These findings emphasize the importance of precipitation timing for grassland ecosystems (Craine, 2013) and the role of climate extreme timing on the ecological response to such extremes (Sippel et al., 2016). Moreover, the observed impacts confirm the findings of Marcolla et al. (2011) indicating that climate conditions at the beginning of the growing season play a crucial role in influencing seasonal and inter-annual variability of canopy functional and structural properties in mountain grasslands.

With this study we add a further example of the importance of phenocams as useful tools to track not only canopy phenology and its inter-annual variations but also to record the impact of specific events, such as climate extremes. Previous authors (Hufkens et al., 2012b; Mizunuma et al., 2013; Menzel et al., 2015) effectively used phenocams to analyze the impact of late spring frosts on the seasonal patterns of greenness and carbon fluxes in temperate deciduous forest species. This study provides a further evidence of the use of phenocams to record and analyze the effect of a different type of climate extreme, such as heat waves, on mountain grasslands.

4.1. The impact on canopy greenness, canopy traits and photosynthetic ecosystem functional properties

The relationship of canopy traits and photosynthetic ecosystem functional properties with GCC has been recently debated by several authors: some studies on broadleaved deciduous trees (*e.g.* Keenan et al., 2014; Yang et al., 2014), found mismatches between canopy greenness and photosynthetic or morphological parameters, while others highlighted that variations in color fractions are directly driven by changes in canopy traits such as pigment concentrations (Wingate et al., 2015), canopy structure (*e.g.* Inoue et al., 2015; Liu et al., 2015b) or photosynthesis (Toomey et al., 2015). The objective of our study is not to analyze the relationship between GCC and canopy traits, but to understand whether the impact of a climate extreme on canopy greenness can be observed also on canopy traits and photosynthetic ecosystem functional properties. To this end we calculate the heat wave impact metrics both on GCC and on various metrics of canopy structure and function to identify, among the latter, the ones that show a response to the climate extreme similar to what was observed for GCC (Fig. 3). All considered canopy traits consistently show reduced peak values and advanced start of senescence. In particular three groups of traits (Fig. 4) are identified according to their response to the climate extreme. One group includes *GCC*, *PRI*, *LAI* and A_{max}. These traits show a peak reduction range of 29–39% and a peak advance range of 32–43 days indicating a homogeneously strong impact of the heat wave. The reason for their similarity can be found in Rossini et al. (2012) and Migliavacca et al. (2011) who demonstrated that PRI, LAI and GCC are highly correlated in the study site. Significant relations and synchrony between GCC and LAI were found also by other authors in different ecosystems (*e.g.* Liu et al., 2015b; Peichl et al., 2014). Focusing on PRI, it is well know that, like GCC (Wingate et al., 2015), its seasonal course is sensitive to chlorophyll/carotenoids ratio (*e.g.* Gamon et al., 2015; Garbulsky et al., 2011) and recent studies highlighted that it can effectively detect drought effects (*e.g.* Vicca et al., 2016; Merlier et al., 2015; Perez-Priego et al., 2015). Lastly, considering A_{max}, Galvagno et al. (2013) reports that in 2011, in response to a different type of climate extreme (*i.e.* early snowmelt), the study site experienced a consistent and significant reduction of LAI, canopy chlorophyll content and A_{max}, highlighting that plant traits and ecosystem functional properties not only are correlated across sites (*e.g.* Feng and Dietze, 2013; Reichstein et al., 2014; Musavi et al., 2016), but coherently react to climate inter-annual variability. This result thus emphasizes that the mountain grassland under investigation is an ecosystem where proxies of structural and functional canopy traits (*i.e. LAI*, *GCC*, *PRI*) and ecosystem functional properties (*i.e.* A_{max}) are tightly linked.

A second group of traits less severely impacted includes α and GT_{biom}. Maximum α values were reduced in 2015 (PR = 21.9%) but the begin of α decrease is not as advanced as GCC (PA = 4 days). This could indicate a temporal mismatch of the factors driving GCC and α seasonal course and a more general weaker relation between α and vegetation indexes. Indeed Balzarolo et al. (2014), analyzing the relation between ecophysiological parameters and hyperspectral reflectance in mountain grasslands, concluded that the relation between vegetation indexes and α is more uncertain (see also Lasslop et al., 2010), site dependent and weaker than the relation with A_{max}. Considering GT_{biom}, peak reduction and advance are respectively 27.7% and 17 days indicating that biomass was impacted less intensively than GCC and traits belonging to the first group. This could be interpreted in light of the findings of several authors demonstrating that the response of productivity to precipitation changes can vary between sites (Estiarte et al., 2016) and can be the result of the interplay of several factors such as annual precipitation sums (Petrie et al., 2016; Gilgen and Buchmann, 2009), rainfall event size (Cherwin and Knapp, 2012) and the temporal connections between warming and soil drying (Fu et al., 2013; De Boeck et al., 2015; Berdanier and Klein, 2011). The third group includes structural and functional properties showing a moderate impact of the heat wave, namely F_{apar}, NDVI and GPP. In this group peak reduction and advance range between 2.1–9.7% and 15–33 days respectively, indicating that these traits experienced a negligible reduction of peak values but still an important modification of their seasonal course through an earlier senescence onset. The main driver of F_{apar} is total phytomass, including both green biomass and brown senescent necromass (Rossini et al., 2012; Sakowska et al., 2016). Thus it is not surprising that F_{apar} peak value is not considerably reduced taking into account that the heat wave impacted GT_{biom} but only slightly affected total phytomass. NDVI too has been demonstrated to not be extremely effective in the detection of drought effects (Vicca et al., 2016; Gu et al., 2007) or canopy structure changes in canopies of moderate to high biomass (Gamon et al., 1995), where NDVI tends to saturate and to be insensitive to necromass (Gitelson, 2004; Mutanga and Skidmore, 2004). The negligible effect detected on seasonal maximum GPP values agrees with previous studies of Brilli et al. (2011) who did not find a substantial reduction of CO_2 exchange in an Austrian mountain grassland during moderately to extremely dry periods and of Wolf et al. (2013) who even detected an increase in GPP in a Swiss mountain grassland after a spring drought. We hypothesize that the negative effect of low soil water content on GPP could have been compensated by the more favorable conditions of other variables such as the radiation regime or by increased nutrient availability due to changes in microbial activities (Gilgen and Buchmann, 2009). While a negligible reduction of seasonal maximum is found, GPP senesced considerably earlier (PA = 15 days). GPP peak advance is however lower than what was observed for GCC and canopy traits belonging to the first group. This delayed response can be explained considering the

findings of Toomey et al. (2015) and Frank et al. (2015) who suggested that photosynthesis seasonal decline generally lags behind canopy greenness decline in deciduous forests and grasslands.

We acknowledge that this study is based only on three years of data but we highlight that it provides a first promising example of using GCC inter-annual variability to track the inter-annual variability of functional and structural canopy traits in response to a climate extreme in grassland ecosystems. Further studies including more sites and exploiting longer time series are needed to test if this hypothesis holds true for a wider range of ecosystems.

4.2. Impacts on plant functional types

The analysis of heat wave impact on forbs and grasses reveals that both plant functional types experienced a similar reduction of maximum greenness, but forbs show an earlier senescence onset and a greater reduction of greenness seasonal course. This lead us to conclude that forbs, mainly composed by *A. montana*, *G. montanum*, *P. aurea*, and *T. alpinum*, are more impacted than grasses, mostly represented by *N. stricta*. The differential heat wave response of the two functional types can be explained by the high variability in physiological drought tolerance existing among grassland species (Craine et al., 2013). With similar results, De Boeck et al. (2015), in a drought and heat manipulation experiment, hypothesized that forbs were more impacted than graminoids probably because of differences in leaf anatomy: broad sub-horizontal forb leaves have a slower heat dissipation than narrow and vertical grass leaves thus exposing forbs species to higher heat stress risks. A second explanation could be found in the protection effect that dead leaves can play on the lower part of *Nardus* tussocks, where green leaves can survive (Körner, 2003). Other reasons could be differences in leaf mass ratio or rooting depth (Oberbauer and Billings, 1981; Jung et al., 2014) and in particular fine root length/leaf area ratio that can vary between grasses and forbs (Vogel et al., 2012).

Being corroborated by previous experimental studies (De Boeck et al., 2015), these results highlight the enormous potential of pixel-level analysis of phenocam images that has been addressed only very recently by few authors (*e.g.* Julitta et al., 2014; Snyder et al., 2016).

4.3. Modeling the contribution of heat and drought on greenness reduction

GCC reduction during the heat wave is effectively modeled with the new proposed formulation of the GSI model including high temperature and soil water content limitation effects. This result expands the findings of Migliavacca et al. (2011): greenness phenology at the study site is regulated by (i) snow and minimum temperature during spring growth (ii) photoperiod and minimum temperature during senescence and (iii) maximum temperature and soil water content in case of summer heat wave. Fig. 6 shows growing season GSI comparing 2015 with the 2013–2014 average. GSI is the multiplicative combination of all limiting factors included in model formulation and it indicates a full limitation (*i.e.* GSI = 0) when all limiting factors are 0 and no limitation (*i.e.* GSI = 1) when all limiting factors are 1. The course of GSI averaged over 2013–2014 shows a progressive reduction of canopy development limitation from May to early July that corresponds to an increase in GCC; in the second half of July, GSI declines resulting in GCC senescence phase. In 2015 GSI decline is advanced and is driven by maximum temperature and soil water content that are the only limiting factors different from 1 (*i.e.* no limitation) in that period. The vertical dashed line in Fig. 6 indicates the date of GCC peak in 2015 thus demonstrating that canopy entered the senescence phase a few days after maximum temperature and soil water content started to concurrently impose a limitation on greenness.

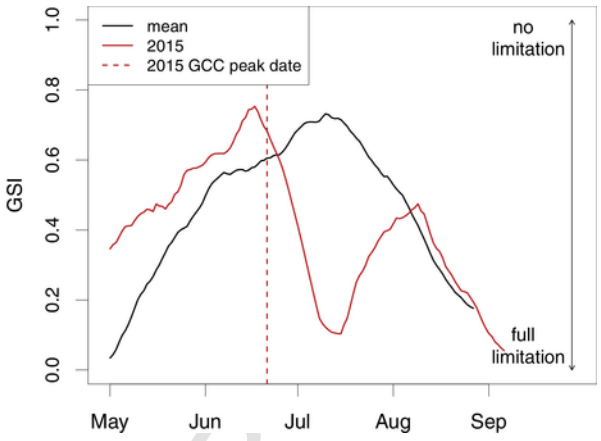

Fig. 6. Growing Season Index (GSI) course resulting from the multiplicative combination of all limiting factors included in model formulation $GSI_{Topt+SWC+Snow}$. GSI ranges from 0 (*i.e.* full limitation of canopy development, all limiting factors = 0) to 1 (*i.e.* no limitation, all limiting factors = 1). Black and red lines represent 2013–2014 mean and 2015 respectively. The red dashed vertical line indicates the occurrence of GCC peak in 2015. (For interpretation of the references to color in this figure legend, the reader is referred to the web version of the article.)

This result is in close agreement with the recent experimental findings by De Boeck et al. (2015) demonstrating that heat waves in combination with drought affected alpine grassland causing early canopy browning. Our results add evidence on the role that high temperature and low soil water content have in co-determining advanced senescence in mountain grasslands and emphasize the importance of hydroclimate variability on autumn phenology, as recently demonstrated by other studies (*e.g.* Liu et al., 2015a; Hwang et al., 2014; Forkel et al., 2015).

5. Conclusions

Climate extremes can play a crucial role in affecting the structure and function of ecosystems. During the long period of high temperature and low soil water content, caused by the record-breaking heat wave scorching Europe in 2015, canopy greenness of a mountain grassland in the Western European Alps was highly impacted: the heat wave hindered the seasonal green wave. Indeed all structural canopy traits and functional ecosystem properties showed a consistent response to the heat wave resulting in a reduction of peak values and anticipated timing of senescence. According to the intensity of their response, three groups of canopy traits were identified: the group most intensively affected included GCC, photosynthetic parameter (A_{max}) and the structural and functional canopy properties (LAI and PRI), while green biomass and α had an intermediate response, and F_{apar}, NDVI and GPP were the least impacted. Moreover exploiting phenocam images at the pixel-level we show that forbs were more impacted than grasses. Finally reformulating the GSI model, we demonstrate that canopy response was driven by the co-limitation of high temperature and low soil moisture. Thus by taking advantage of the natural occurrence of a climate extreme, our results further confirm that mountain grasslands can be profoundly impacted by heat waves in combination with droughts.

Acknowledgments

The present work was supported by ePheno and Tourscience projects (cofunded by the European Regional Developmental Fund, ALCOTRA 2007–2013 and 2014–2020) and the NextData Data-LTER-Mountain project. We thank the anonymous reviewers for their comments that substantially improved the manuscript.

References

Akaike, H., 1992. Information theory and an extension of the maximum likelihood principle. Breakthroughs in Statistics. Springer, 610–624.

Bahn, M., Reichstein, M., Dukes, J., 2014. Climate biosphere interactions in a more extreme world. New Phytol. https://doi.org/10.1111/nph.12662.

Balzarolo, M., Vescovo, L., Hammerle, A., Gianelle, D., Papale, D., Wohlfahrt, G., 2014. On the relationship between ecosystem-scale hyperspectral reflectance and CO_2 exchange in European mountain grasslands. Biogeosciences 11, 10323–10363. https://doi.org/10.5194/bgd-11-10323-2014 http://www.biogeosciences-discuss.net/11/10323/2014/bgd-11-10323-2014.html.

Beniston, M., 2012. Impacts of climatic change on water and associated economic activities in the Swiss Alps. J. Hydrol. 412–413, 291–296. https://doi.org/10.1016/j.jhydrol.2010.06.046 http://linkinghub.elsevier.com/retrieve/pii/S0022169410004993.

Berdanier, A.B., Klein, J.A., 2011. Growing season length and soil moisture interactively constrain high elevation aboveground net primary production. Ecosystems 14, 963–974. https://doi.org/10.1007/s10021-011-9459-1.

Brilli, F., Hörtnagl, L., Hammerle, A., Haslwanter, A., Hansel, A., Loreto, F., Wohlfahrt, G., 2011. Leaf and ecosystem response to soil water availability in mountain grasslands. Agric. For. Meteorol. 151, 1731–1740. https://doi.org/10.1016/j.agrformet.2011.07.007.

Brown, T., Hultine, K., Steltzer, H., Denny, E., Denslow, M., Granados, J., Henderson, S., Moore, D., Nagai, S., San Clements, M., Sánchez-Azofeifa, A., Sonnentag, O., Tazik, D., Richardson, A., 2016. Using phenocams to monitor our changing Earth: towards a global phenocam network. Front. Ecol. Environ. https://doi.org/10.1002/12.0207.1, (in press).

Buitenwerf, R., Rose, L., Higgins, S.I., 2015. Three decades of multi-dimensional change in global leaf phenology. Nat. Clim. Change https://doi.org/10.1038/nclimate2533, (advance on).

CaraDonna, P.J., Inouye, D.W., 2015. Phenological responses to climate change do not exhibit phylogenetic signal in a subalpine plant community. Ecology 96, 355–361. https://doi.org/10.1890/14-1536.1.

Cherwin, K., Knapp, A., 2012. Unexpected patterns of sensitivity to drought in three semi-arid grasslands. Oecologia 169, 845–852. https://doi.org/10.1007/s00442-011-2235-2.

Choler, P., 2015. Growth Response of Temperate Mountain Grasslands to Inter-annual Variations of Snow Cover Duration. http://biogeosciences-discuss.net/12/3025/2015/bgd-12-3025-2015.pdf.

Ciais, P., Reichstein, M., Viovy, N., Granier, A., Ogée, J., Allard, V., Aubinet, M., Buchmann, N., Bernhofer, C., Carrara, A., Chevallier, F., De Noblet, N., Friend, A.D., Friedlingstein, P., Grünwald, T., Heinesch, B., Keronen, P., Knohl, A., Krinner, G., Loustau, D., Manca, G., Matteucci, G., Miglietta, F., Ourcival, J.M., Papale, D., Pilegaard, K., Rambal, S., Seufert, G., Soussana, J.F., Sanz, M.J., Schulze, E.D., Vesala, T., Valentini, R., 2005. Europe-wide reduction in primary productivity caused by the heat and drought in 2003. Nature 437, 529–533. https://doi.org/10.1038/nature03972.

Craine, J.M., 2013. The importance of precipitation timing for grassland productivity. Plant Ecol. 214, 1085–1089. https://doi.org/10.1007/s11258-013-0236-4.

Craine, J.M., Ocheltree, T.W., Nippert, J.B., Towne, E.G., Skibbe, A.M., Kembel, S.W., Fargione, J.E., 2013. Global diversity of drought tolerance and grassland climate-change resilience. Nat. Clim. Change 3, 63–67. https://doi.org/10.1038/nclimate1634 http://www.nature.com/nclimate/journal/v3/n1/full/nclimate1634.html.

De Boeck, H.J., Bassin, S., Verlinden, M., Zeiter, M., Hiltbrunner, E., 2015. Simulated heat waves affected alpine grassland only in combination with drought. New Phytol. https://doi.org/10.1111/nph.13601.

Eklundh, L., Jin, H., Schubert, P., Guzinski, R., Heliasz, M., 2011. An Optical Sensor Network for Vegetation Phenology Monitoring and Satellite Data Calibration, vol. 11, https://doi.org/10.3390/s110807678 http://www.pubmedcentral.nih.gov/articlerender.fcgi?artid=3231725&tool=pmcentrez&rendertype=abstract.

Ernakovich, J.G., Hopping, K.A., Berdanier, A.B., Simpson, R.T., Kachergis, E.J., Steltzer, H., Wallenstein, M.D., 2014. Predicted responses of arctic and alpine ecosystems to altered seasonality under climate change. Glob. Change Biol. https://doi.org/10.1111/gcb.12568 http://www.ncbi.nlm.nih.gov/pubmed/24599697.

Estiarte, M., Vicca, S., Penuelas, J., Bahn, M., Beier, C., Emmett, B.A., Fay, P.A., Hanson, P.J., Hasibeder, R., Kigel, J., Kroel-Dulay, G., Larsen, K.S., Lellei-Kovacs, E., Limousin, J.M., Ogaya, R., Ourcival, J.M., Reinsch, S., Sala, O.E., Schmidt, I.K., Sternberg, M., Tielboerger, K., Tietema, A., Janssens, I.A., 2016. Few multiyear precipitation–reduction experiments find a shift in the productivity-precipitation relationship. Glob. Change Biol. 22, 2570–2581. https://doi.org/10.1111/gcb.13269.

Falge, E., Baldocchi, D., Olson, R., Anthoni, P., Aubinet, M., Bernhofer, C., Burba, G., Ceulemans, R., Clement, R., Dolman, H., Granier, A., Gross, P., Grünwald, T., Hollinger, D., Jensen, N.O., Katul, G., Keronen, P., Kowalski, A., Lai, C.T., Law, B.E., Meyers, T., Moncrieff, J., Moors, E., Munger, J.W., Pilegaard, K., Rannik, L., Rebmann, C., Suyker, A., Tenhunen, J., Tu, K., Verma, S., Vesala, T., Wilson, K., Wofsy, S., 2001. Gap filling strategies for defensible annual sums of net ecosystem exchange. Agric. For. Meteorol. 107, 43–69. https://doi.org/10.1016/S0168-1923(00)00225-2.

Feng, X., Dietze, M., 2013. Scale dependence in the effects of leaf ecophysiological traits on photosynthesis: Bayesian parameterization of photosynthesis models. New Phytol. 200, 1132–1144. https://doi.org/10.1111/nph.12454.

Filippa, G., Cremonese, E., Galvagno, M., Migliavacca, M., Morra di Cella, U., Petey, M., Siniscalco, C., 2015. Five years of phenological monitoring in a mountain grassland: inter-annual patterns and evaluation of the sampling protocol. Int. J. Biometeorol. https://doi.org/10.1007/s00484-015-0999-5.

Filippa, G., Cremonese, E., Migliavacca, M., Galvagno, M., Forkel, M., Wingate, L., Tomelleri, E., Morra di Cella, U., Richardson, A.D., 2016. Phenopix: a R package for image-based vegetation phenology. Agric. For. Meteorol. 220, 141–150. https://doi.org/10.1016/j.agrformet.2016.01.006 http://linkinghub.elsevier.com/retrieve/pii/S0168192316300089.

Forkel, M., Migliavacca, M., Thonicke, K., Reichstein, M., Schaphoff, S., Weber, U., Carvalhais, N., 2015. Codominant water control on global interannual variability and trends in land surface phenology and greenness. Glob. Change Biol. 21, 3414–3435. https://doi.org/10.1111/gcb.12950.

Frank, D., Reichstein, M., Bahn, M., Thonicke, K., Frank, D., Mahecha, M.D., Smith, P., van der Velde, M., Vicca, S., Babst, F., Beer, C., Buchmann, N., Canadell, J.G., Ciais, P., Cramer, W., Ibrom, A., Miglietta, F., Poulter, B., Rammig, A., Seneviratne, S.I., Walz, A., Wattenbach, M., Zavala, M.A., Zscheischler, J., 2015. Effects of climate extremes on the terrestrial carbon cycle: concepts, processes and potential future impacts. Glob. Change Biol. 21, 2861–2880. https://doi.org/10.1111/gcb.12916.

Fu, G., Zhang, X.Z., Zhang, Y.J., Shi, P.L., Li, Y.L., Zhou, Y.T., Yang, P.W., Shen, Z.X., 2013. Experimental warming does not enhance gross primary production and above-ground biomass in the alpine meadow of Tibet. J. Appl. Remote Sens. 7, 73505. https://doi.org/10.1117/1.JRS.7.073505.

Fu, Y.H., Zhao, H., Piao, S., Peaucelle, M., Peng, S., Zhou, G., Ciais, P., Huang, M., Menzel, A., Pe nuelas, J., Song, Y., Vitasse, Y., Zeng, Z., Janssens, I.A., 2015. Declining global warming effects on the phenology of spring leaf unfolding. Nature https://doi.org/10.1038/nature15402.

Fuchslueger, L., Bahn, M., Fritz, K., Hasibeder, R., Richter, A., 2014. Experimental drought reduces the transfer of recently fixed plant carbon to soil microbes and alters the bacterial community composition in a mountain meadow. New Phytol. 201, 916–927. https://doi.org/10.1111/nph.12569.

Galvagno, M., Wohlfahrt, G., Cremonese, E., Filippa, G., Migliavacca, M., di Cella, U.M., van Gorsel, E., 2017. Contribution of advection to nighttime ecosystem respiration at a mountain grassland in complex terrain. Agric. For. Meteorol. 237, 270–281.

Galvagno, M., Wohlfahrt, G., Cremonese, E., Rossini, M., Colombo, R., Filippa, G., Julitta, T., Manca, G., Siniscalco, C., di Cella, U.M., Migliavacca, M., 2013. Phenology and carbon dioxide source/sink strength of a subalpine grassland in response to an exceptionally short snow season. Environ. Res. Lett. 8, 25008 http://stacks.iop.org/1748-9326/8/i=2/a=025008.

Gamon, J.A., Field, C.B., Goulden, M.L., Griffin, K.L., Hartley, A.E., Joel, G., Penuelas, J., Valentini, R., 1995. Relationships between NDVI, canopy structure, and photosynthesis in three Californian vegetation types. Ecol. Appl. 5, 28–41. https://doi.org/10.2307/1942049.

Gamon, J.A., Kovalchuck, O., Wong, C.Y.S., Harris, A., Garrity, S.R., 2015. Monitoring seasonal and diurnal changes in photosynthetic pigments with automated PRI and NDVI sensors. Biogeosciences 12, 4149–4159. https://doi.org/10.5194/bg-12-4149-2015 http://www.biogeosciences.net/12/4149/2015/.

Gamon, J.A., Serrano, L., Surfus, J.S., 1997. The photochemical reflectance index: an optical indicator of photosynthetic radiation use efficiency across species, functional types, and nutrient levels. Oecologia 112, 492–501. https://doi.org/10.1007/s004420050337.

Garbulsky, M.F., Peñuelas, J., Gamon, J., Inoue, Y., Filella, I., 2011. The photochemical reflectance index (PRI) and the remote sensing of leaf, canopy and ecosystem radiation use efficiencies. A review and meta-analysis. Remote Sens. Environ. 115, 281–297. https://doi.org/10.1016/j.rse.2010.08.023.

García-Herrera, R., Díaz, J., Trigo, R., Luterbacher, J., Fischer, E., 2010. A review of the European summer heat wave of 2003. Crit. Rev. Environ. Sci. Technol. 40, 267–306.

Gilgen, A.K., Buchmann, N., 2009. Response of temperate grasslands at different altitudes to simulated summer drought differed but scaled with annual precipitation. Biogeosciences 6, 2525–2539. https://doi.org/10.5194/bg-6-2525-2009.

Gitelson, A.A., 2004. Wide dynamic range vegetation index for remote quantification of biophysical characteristics of vegetation. J. Plant Physiol. 161, 165–173. https://doi.org/10.1078/0176-1617-01176.

Gobiet, A., Kotlarski, S., Beniston, M., Heinrich, G., Rajczak, J., Stoffel, M., 2013. 21st century climate change in the European Alps – a review. Sci. Total Environ. https://doi.org/10.1016/j.scitotenv.2013.07.050 http://linkinghub.elsevier.com/retrieve/pii/S0048969713008188.

Gu, L., Post, W.M., Baldocchi, D.D., Black, T.A., Suyker, A.E., Verma, S.B., Vesala, T., Wofsy, S.C., 2009. Characterizing the seasonal dynamics of plant community photosynthesis across a range of vegetation types. Phenology of Ecosystem Processes. Springer, 35–58.

Gu, Y., Brown, J.F., Verdin, J.P., Wardlow, B., 2007. A five-year analysis of MODIS NDVI and NDWI for grassland drought assessment over the central Great Plains of the United States. Geophys. Res. Lett. 34, L06407. https://doi.org/10.1029/2006GL029127.

Haario, H., Laine, M., Mira, A., Saksman, E., 2006. DRAM: efficient adaptive MCMC. Stat. Comput. 16, 339–354. https://doi.org/10.1007/s11222-006-9438-0.

Heffernan, O., 2016. Climate research is gaining ground. Nat. Clim. Change 6, 335–338. https://doi.org/10.1038/nclimate2974.

Hoover, D.L., Knapp, A.K., Smith, M.D., 2014. Resistance and resilience of a grassland ecosystem to climate extremes. Ecology 95, 2646–2656. https://doi.org/10.1890/13-2186.1.

Hufkens, K., Friedl, M., Sonnentag, O., Braswell, B.H., Milliman, T., Richardson, A.D., 2012. Linking near-surface and satellite remote sensing measurements of deciduous broadleaf forest phenology. Remote Sens. Environ. 117, 307–321. https://doi.org/10.1016/j.rse.2011.10.006 http://linkinghub.elsevier.com/retrieve/pii/S0034425711003543.

Hufkens, K., Friedl, M.A., Keenan, T.F., Sonnentag, O., Bailey, A., O'Keefe, J., Richardson, A.D., 2012. Ecological impacts of a widespread frost event following early spring leaf-out. Glob. Change Biol. 18, 2365–2377. https://doi.org/10.1111/j.1365-2486.2012.02712.x.

Hufkens, K., Keenan, T.F., Flanagan, L.B., Scott, R.L., Bernacchi, C.J., Joo, E., Brunsell, N.A., Verfaillie, J., Richardson, A.D., 2016. Productivity of North American grasslands is increased under future climate scenarios despite rising aridity. Nat. Clim. Change 04, 1–18. https://doi.org/10.1038/nclimate2942.

Hwang, T., Band, L.E., Miniat, C.F., Song, C., Bolstad, P.V., Vose, J.M., Love, J.P., 2014. Divergent phenological response to hydroclimate variability in forested mountain watersheds. Glob. Change Biol. 20, 2580–2595. https://doi.org/10.1111/gcb.12556 http://www.ncbi.nlm.nih.gov/pubmed/24677382.

Inoue, T., Nagai, S., Kobayashi, H., Koizumi, H., 2015. Utilization of ground-based digital photography for the evaluation of seasonal changes in the aboveground green biomass and foliage phenology in a grassland ecosystem. Ecol. Inform. 25, 1–9. https://doi.org/10.1016/j.ecoinf.2014.09.013.

IPCC, 2013. Climate Change 2013: The Physical Science Basis. Contribution of Working Group I to the Fifth Assessment Report of the Intergovernmental Panel on Climate Change. Cambridge University Press, Cambridge, United Kingdom and New York, NY, USA, https://doi.org/10.1017/CBO9781107415324 www.climatechange2013.org.

Janssen, P., Heuberger, P., 1995. Calibration of process-oriented models. Ecol. Model. 83, 55–66.

Jolly, W.M., Nemani, R., Running, S.W., 2005. A generalized, bioclimatic index to predict foliar phenology in response to climate. Glob. Change Biol. 11, 619–632. https://doi.org/10.1111/j.1365-2486.2005.00930.x.

Julitta, T., Cremonese, E., Migliavacca, M., Colombo, R., Galvagno, M., Siniscalco, C., Rossini, M., Fava, F., Cogliati, S., Morra di Cella, U., Menzel, A., 2014. Using digital camera images to analyse snowmelt and phenology of a subalpine grassland. Agric. For. Meteorol. 198–199, 116–125.

Jung, V., Albert, C.H., Violle, C., Kunstler, G., Loucougaray, G., Spiegelberger, T., 2014. Intraspecific trait variability mediates the response of subalpine grassland communities to extreme drought events. J. Ecol. 102, 45–53. https://doi.org/10.1111/1365-2745.12177.

Kaufman, L., Rousseeuw, P., 1987. Clustering by Means of Medoids. North-Holland.

Keenan, T.F., Darby, B., Felts, E., Sonnentag, O., Friedl, M., Hufkens, K., O'Keefe, J.F., Klosterman, S., Munger, J.W., Toomey, M., Richardson, A.D., 2014. Tracking forest phenology and seasonal physiology using digital repeat photography: a critical assessment. Ecol. Appl. https://doi.org/10.1890/13-0652.1, 140206175103002.

Klosterman, S.T., Hufkens, K., Gray, J.M., Melaas, E., Sonnentag, O., Lavine, I., Mitchell, L., Norman, R., Friedl, M.A., Richardson, A.D., 2014. Evaluating remote sensing of deciduous forest phenology at multiple spatial scales using PhenoCam imagery. Biogeosciences 11, 4305–4320.

Knox, S.H., Dronova, I., Sturtevant, C., Oikawa, P.Y., Matthes, J.H., Verfaillie, J., Baldocchi, D., 2017. Using digital camera and Landsat imagery with eddy covariance data to model gross primary production in restored wetlands. Agric. For. Meteorol. 237, 233–245. https://doi.org/10.1016/j.agrformet.2017.02.020.

Körner, C., 2003. Alpine Plant Life: Functional Plant Ecology of High Mountain Ecosystems; with 47 Tables. Springer Science & Business Media.

Kreyling, J., Jentsch, A., Beier, C., 2014. Beyond realism in climate change experiments: gradient approaches identify thresholds and tipping points. Ecol. Lett. 17, https://doi.org/10.1111/ele.12193, 125.e1.

Kreyling, J., Jentsch, A., Beierkuhnlein, C., 2011. Stochastic trajectories of succession initiated by extreme climatic events. Ecol. Lett. 14, 758–764. https://doi.org/10.1111/j.1461-0248.2011.01637.x.

Lasslop, G., Reichstein, M., Papale, D., Richardson, A.D., Arneth, A., Barr, A., Stoy, P., Wohlfahrt, G., 2010. Separation of net ecosystem exchange into assimilation and respiration using a light response curve approach: critical issues and global evaluation. Glob. Change Biol. 16, 187–208. https://doi.org/10.1111/j.1365-2486.2009.02041.x.

Liu, Q., Fu, Y.H., Zeng, Z., Huang, M., Li, X., Piao, S., 2015. Temperature, precipitation, and insolation effects on autumn vegetation phenology in temperate China. Glob. Change Biol.https://doi.org/10.1111/gcb.13081 http://www.ncbi.nlm.nih.gov/pubmed/26340580.

Liu, Z., Hu, H., Yu, H., Yang, X., Yang, H., Ruan, C., Wang, Y., 2015. Relationship between leaf physiologic traits and canopy color indices during the leaf expansion period in an oak forest. Ecosphere 6, 1–9. https://doi.org/10.1890/ES14-00452.1.

Maechler, M., Rousseeuw, P., Struyf, A., Hubert, M., Hornik, K., 2016. cluster: Cluster Analysis Basics and Extensions. R Package Version 2.0.4 — For New Features, See the 'Changelog' File (in the Package Source).

Marcolla, B., Cescatti, A., Manca, G., Zorer, R., Cavagna, M., Fiora, A., Gianelle, D., Rodeghiero, M., Sottocornola, M., Zampedri, R., 2011. Climatic controls and ecosystem responses drive the inter-annual variability of the net ecosystem exchange of an alpine meadow. Agric. For. Meteorol. 151, 1233–1243. https://doi.org/10.1016/j.agrformet.2011.04.015 http://linkinghub.elsevier.com/retrieve/pii/S0168192311001444.

Menzel, A., Helm, R., Zang, C., 2015. Patterns of late spring frost leaf damage and recovery in a European beech (Fagus sylvatica L.) stand in south-eastern Germany based on repeated digital photographs. Front. Plant Sci. 6, 110. https://doi.org/10.3389/fpls.2015.00110.

Menzel, A., Sparks, T., Estrella, N., Koch, E., Aasa, A., Ahas, R., Alm-kubler, K., Bissolli, P., Braslavska, O., Briede, A., Chmielewski, F., Crepinsek, Z., Curnell, Y., Dahl, A., Defila, C., Donnelly, A., Filella, I., Jatczak, K., Mage, F., Mestre, A., Nordli, O., Penuelas, J., Pirinen, P., Remisova, V., Scheifinger, H., Striz, M., Susnik, A., Van Liet, A., Wiegolaski, F.E., Zach, S., Zust, A., 2006. European phenological response to climate change matches the warming pattern. Glob. Change Biol. 12, 1969–1976. https://doi.org/10.1111/j.1365-2486.2006.01193.x.

Merlier, E., Hmimina, G., Dufrêne, E., Soudani, K., 2015. Explaining the variability of the photochemical reflectance index (PRI) at the canopy-scale: disentangling the effects of phenological and physiological changes. J. Photochem. Photobiol. B: Biol. 151, 161–171. https://doi.org/10.1016/j.jphotobiol.2015.08.006 http://linkinghub.elsevier.com/retrieve/pii/S1011134415002468.

Migliavacca, M., Galvagno, M., Cremonese, E., Rossini, M., Meroni, M., Sonnentag, O., Cogliati, S., Manca, G., Diotri, F., Busetto, L., Cescatti, A., Colombo, R., Fava, F., Morra di Cella, U., Pari, E., Siniscalco, C., Richardson, A.D., 2011. Using digital repeat photography and eddy covariance data to model grassland phenology and photosynthetic CO_2 uptake. Agric. For. Meteorol. 151, 1325–1337. https://doi.org/10.1016/j.agrformet.2011.05.012.

Migliavacca, M., Sonnentag, O., Keenan, T.F., Cescatti, A., O'Keefe, J., Richardson, A.D., 2012. On the uncertainty of phenological responses to climate change, and implications for a terrestrial biosphere model. Biogeosciences 9, 2063–2083. https://doi.org/10.5194/bg-9-2063-2012.

Mizunuma, T., Wilkinson, M., Eaton, E.L., Mencuccini, M., Morison, J.I.L., Grace, J., 2013. The relationship between carbon dioxide uptake and canopy colour from two camera systems in a deciduous forest in southern England. Funct. Ecol. 27, 196–207. https://doi.org/10.1111/1365-2435.12026.

Musavi, T., Migliavacca, M., van de Weg, M.J., Kattge, J., Wohlfahrt, G., van Bodegom, P.M., Reichstein, M., Bahn, M., Carrara, A., Domingues, T.F., Gavazzi, M., Gianelle, D., Gimeno, C., Granier, A., Gruening, C., Havránková, K., Herbst, M., Hrynkiw, C., Kalhori, A., Kaminski, T., Klumpp, K., Kolari, P., Longdoz, B., Minerbi, S., Montagnani, L., Moors, E., Oechel, W.C., Reich, P.B., Rohatyn, S., Rossi, A., Rotenberg, E., Varlagin, A., Wilkinson, M., Wirth, C., Mahecha, M.D., 2016. Potential and limitations of inferring ecosystem photosynthetic capacity from leaf functional traits. Ecol. Evol. 6, 7352–7366. https://doi.org/10.1002/ece3.2479.

Mutanga, O., Skidmore, A.K., 2004. Narrow band vegetation indices overcome the saturation problem in biomass estimation. Int. J. Remote Sens. 25, 3999–4014. https://doi.org/10.1080/01431160310001654923.

Nagai, S., Maeda, T., Gamo, M., Muraoka, H., Suzuki, R., Nasahara, K.N., 2011. Using digital camera images to detect canopy condition of deciduous broad-leaved trees. Plant Ecol. Divers. 4, 79–89. https://doi.org/10.1080/17550874.2011.579188.

Nagler, P.L., Pearlstein, S., Glenn, E.P., Brown, T.B., Bateman, H.L., Bean, D.W., Hultine, K.R., 2014. Rapid dispersal of saltcedar (Tamarix spp.) biocontrol beetles (Diorhabda carinulata) on a desert river detected by phenocams, MODIS imagery and ground observations. Remote Sens. Environ. 140, 206–219. https://doi.org/10.1016/j.rse.2013.08.017.

Nasahara, K., Nagai, S., 2015. Review: Development of an in-situ observation network for terrestrial ecological remote sensing – the Phenological Eyes Network (PEN). Ecol. Res. 30, 211–223. https://doi.org/10.1007/s11284-014-1239-x.

Oberbauer, S.F., Billings, W.D., 1981. Drought tolerance and water use by plants along an alpine elevational gradient. Oecologia 50, 325–331.

Olofsson, P., Eklundh, L., 2007. Estimation of absorbed par across scandinavia from satellite measurements. Part II: Modeling and evaluating the fractional absorption. Remote Sens. Environ. 110, 240–251.

Peichl, M., Sonnentag, O., Nilsson, M.B., 2014. Bringing color into the picture: using digital repeat photography to investigate phenology controls of the carbon dioxide exchange in a boreal mire. Ecosystems https://doi.org/10.1007/s10021-014-9815-z.

Peichl, M., Sonnentag, O., Wohlfahrt, G., Flanagan, L.B., Baldocchi, D.D., Kiely, G., Galvagno, M., Gianelle, D., Marcolla, B., Pio, C., Migliavacca, M., Jones, M.B., Saunders, M., 2013. Convergence of potential net ecosystem production among contrasting C3 grasslands. Ecol. Lett. 16, 502–512. https://doi.org/10.1111/ele.12075 http://www.ncbi.nlm.nih.gov/pubmed/23346985.

Perez-Priego, O., Guan, J., Rossini, M., Fava, F., Wutzler, T., Moreno, G., Carvalhais, N., Carrara, A., Kolle, O., Julitta, T., Schrumpf, M., Reichstein, M., Migliavacca, M., 2015. Sun-induced chlorophyll fluorescence and photochemical reflectance index improve remote-sensing gross primary production estimates under varying nutrient availability in a typical Mediterranean savanna

ecosystem. Biogeosciences 12, 6351–6367. https://doi.org/10.5194/bg-12-6351-2015.
Petrie, M.D., Brunsell, N.A., Vargas, R., Collins, S.L., Flanagan, L.B., Hanan, N.P., Litvak, M.E., Suyker, A.E., 2016. The sensitivity of carbon exchanges in Great Plains grasslands to precipitation variability. J. Geophys. Res.: Biogeosci. https://doi.org/10.1002/2015JG003205.
Pintaldi, E., D'Amico, M.E., Siniscalco, C., Cremonese, E., Celi, L., Filippa, G., Prati, M., Freppaz, M., 2016. Hummocks affect soil properties and soil-vegetation relationships in a subalpine grassland (North-Western Italian Alps). Catena 145, 214–226. https://doi.org/10.1016/j.catena.2016.06.014 http://linkinghub.elsevier.com/retrieve/pii/S0341816216302193.
R Core Team, 2015. R: A Language and Environment for Statistical Computing. R Foundation for Statistical Computing, Vienna, Austria http://www.r-project.org/.
Rammig, A., Wiedermann, M., Donges, J.F., Babst, F., Von Bloh, W., Frank, D., Thonicke, K., Mahecha, M.D., 2015. Coincidences of climate extremes and anomalous vegetation responses: comparing tree ring patterns to simulated productivity. Biogeosciences 12, 373–385. https://doi.org/10.5194/bg-12-373-2015.
Reichstein, M., Bahn, M., Ciais, P., Frank, D., Mahecha, M.D., Seneviratne, S.I., Zscheischler, J., Beer, C., Buchmann, N., Frank, D.C., Papale, D., Rammig, A., Smith, P., Thonicke, K., van der Velde, M., Vicca, S., Walz, A., Wattenbach, M., 2013. Climate extremes and the carbon cycle. Nature 500, 287–295. https://doi.org/10.1038/nature12350 http://www.ncbi.nlm.nih.gov/pubmed/23955228.
Reichstein, M., Bahn, M., Mahecha, M.D., Kattge, J., Baldocchi, D.D., 2014. Linking plant and ecosystem functional biogeography. Proc. Natl. Acad. Sci. U. S. A. 111, https://doi.org/10.1073/pnas.1216065111, 201216065, http://www.pnas.org/content/early/2014/09/10/1216065111, http://www.ncbi.nlm.nih.gov/pubmed/25225392, http://www.pnas.org/content/early/2014/09/10/1216065111.abstract.
Reichstein, M., Subke, J.A., Angeli, A.C., Tenhunen, J.D., 2005. Does the temperature sensitivity of decomposition of soil organic matter depend upon water content, soil horizon, or incubation time?. Glob. Change Biol. 11, 1754–1767. https://doi.org/10.1111/j.1365-2486.2005.01010.x.
Reyer, C.P.O., Leuzinger, S., Rammig, A., Wolf, A., Bartholomeus, R.P., Bonfante, A., de Lorenzi, F., Dury, M., Gloning, P., Abou Jaoudé, R., Klein, T., Kuster, T.M., Martins, M., Niedrist, G., Riccardi, M., Wohlfahrt, G., de Angelis, P., de Dato, G., François, L., Menzel, A., Pereira, M., 2013. A plant's perspective of extremes: terrestrial plant responses to changing climatic variability. Glob. Change Biol. 19, 75–89. https://doi.org/10.1111/gcb.12023 http://www.pubmedcentral.nih.gov/articlerender.fcgi?artid=3857548&tool=pmcentrez&rendertype=abstract.
Reynolds, A.P., Richards, G., de la Iglesia, B., Rayward-Smith, V.J., 2006. Clustering rules: a comparison of partitioning and hierarchical clustering algorithms. J. Math. Model. Algorithms 5, 475–504.
Richardson, A.D., Hollinger, D.Y., Dail, D.B., Lee, J.T., Munger, J.W., O'keefe, J., 2009. Influence of spring phenology on seasonal and annual carbon balance in two contrasting New England forests. Tree Physiol. 29, 321–331. https://doi.org/10.1093/treephys/tpn040.
Richardson, A.D., Jenkins, J.P., Braswell, B.H., Hollinger, D.Y., Ollinger, S.V., Smith, M.L., 2007. Use of digital webcam images to track spring green-up in a deciduous broadleaf forest. Oecologia 152, 323–334. https://doi.org/10.1007/s00442-006-0657-z http://www.ncbi.nlm.nih.gov/pubmed/17342508.
Richardson, A.D., Keenan, T.F., Migliavacca, M., Ryu, Y., Sonnentag, O., Toomey, M., 2013. Climate change, phenology, and phenological control of vegetation feedbacks to the climate system. Agric. For. Meteorol. 169, 156–173. https://doi.org/10.1016/j.agrformet.2012.09.012 http://linkinghub.elsevier.com/retrieve/pii/S0168192312002869.
Rossini, M., Cogliati, S., Meroni, M., Migliavacca, M., Galvagno, M., Busetto, L., Cremonese, E., Julitta, T., Siniscalco, C., Morra Di Cella, U., Colombo, R., 2012. Remote sensing-based estimation of gross primary production in a subalpine grassland. Biogeosciences 9, 2565–2584.
Rouse, J., Haas, R., Schell, J., Deering, D., 1974. Monitoring Vegetation Systems in the Great Plains with Erts. NASA Special Publication 351. 309.
Saitoh, T.M., Nagai, S., Saigusa, N., Kobayashi, H., Suzuki, R., Nasahara, K.N., Muraoka, H., 2012. Assessing the use of camera-based indices for characterizing canopy phenology in relation to gross primary production in a deciduous broad-leaved and an evergreen coniferous forest in Japan. Ecol. Inform. 11, 45–54. https://doi.org/10.1016/j.ecoinf.2012.05.001 http://linkinghub.elsevier.com/retrieve/pii/S1574954112000416.
Sakamoto, T., Gitelson, A.A., Nguy-Robertson, A.L., Arkebauer, T.J., Wardlow, B.D., Suyker, A.E., Verma, S.B., Shibayama, M., 2012. An alternative method using digital cameras for continuous monitoring of crop status. Agric. For. Meteorol. 154–155, 113–126. https://doi.org/10.1016/j.agrformet.2011.10.014 http://linkinghub.elsevier.com/retrieve/pii/S0168192311003133.
Sakowska, K., Juszczak, R., Gianelle, D., 2016. Remote sensing of grassland biophysical parameters in the context of the Sentinel-2 satellite mission. J. Sens. 2016, https://doi.org/10.1155/2016/4612809, 16 pp..
Scheffers, B.R., De Meester, L., Bridge, T.C.L., Hoffmann, A.A., Pandolfi, J.M., Corlett, R.T., Butchart, S.H.M., Pearce-Kelly, P., Kovacs, K.M., Dudgeon, D., Pacifici, M., Rondinini, C., Foden, W.B., Martin, T.G., Mora, C., Bickford, D., Watson, J.E.M., 2016. The broad footprint of climate change from genes to biomes to people. Science 354.
Schwartz, M.D., 1998. Green wave phenology. Nature 394, 839. https://doi.org/10.1038/29667.
Seddon, A.W.R., Macias-Fauria, M., Long, P.R., Benz, D., Willis, K.J., 2016. Sensitivity of global terrestrial ecosystems to climate variability. Nature https://doi.org/10.1038/nature16986, (advance on).
Sippel, S., Zscheischler, J., Reichstein, M., 2016. Ecosystem impacts of climate extremes crucially depend on the timing. Proc. Natl. Acad. Sci. U. S. A. https://doi.org/10.1073/pnas.1605667113, 201605667.
Smith, M.D., 2011. An ecological perspective on extreme climatic events: a synthetic definition and framework to guide future research. J. Ecol. 99, 656–663. https://doi.org/10.1111/j.1365-2745.2011.01798.x.
Snyder, K.A., Wehan, B.L., Filippa, G., Huntington, J.L., Stringham, T.K., Snyder, D.K., 2016. Extracting plant phenology metrics in a great basin watershed: methods and considerations for quantifying phenophases in a cold desert. Sensors (Switzerland) 16, https://doi.org/10.3390/s16111948.
Sonnentag, O., Hufkens, K., Teshera-Sterne, C., Young, A.M., Friedl, M., Braswell, B.H., Milliman, T., O'Keefe, J., Richardson, A.D., 2012. Digital repeat photography for phenological research in forest ecosystems. Agric. For. Meteorol. 152, 159–177. https://doi.org/10.1016/j.agrformet.2011.09.009 http://linkinghub.elsevier.com/retrieve/pii/S0168192311002851.
Tollefson, J., 2015. 2015 breaks heat record. Nature 529, 450. https://doi.org/10.1038/nature.2016.19216.
Toomey, M., Friedl, M., Frolking, S., 2015. Greenness indices from digital cameras predict the timing and seasonal dynamics of canopy-scale photosynthesis. Ecol. Appl. 25, 99–115 http://dash.harvard.edu/handle/1/13575368.
Vicca, S., Balzarolo, M., Filella, I., Granier, A., Herbst, M., Knohl, A., Longdoz, B., Mund, M., Nagy, Z., Pintér, K., Rambal, S., Verbesselt, J., Verger, A., Zeileis, A., Zhang, C., Pe nuelas, J., 2016. Detection of effects of extreme droughts on gross primary production using satellite data. Sci. Rep. https://doi.org/10.1038/srep28269.
Vitasse, Y., Rebetez, M., Filippa, G., Cremonese, E., Klein, G., Rixen, C., 2016. Hearing alpine plants growing after snowmelt: ultrasonic snow sensors provide long-term series of alpine plant phenology. Int. J. Biometeorol. 1–13. https://doi.org/10.1007/s00484-016-1216-x.
Vogel, A., Scherer-Lorenzen, M., Weigelt, A., Jacob, D., Göttel, H., Kotlarski, S., Lorenz, P., Sieck, K., Hector, A., Bagchi, R., Isbell, F., Calcagno, V., Hector, A., Connolly, J., Harpole, W., Hector, A., Schmid, B., Beierkuhnlein, C., Caldeira, M., Diemer, M., Tilman, D., Reich, P., Knops, J., Wedin, D., Mielke, T., van Ruijven, J., Berendse, F., Marquard, E., Weigelt, A., Temperton, V., Roscher, C., Schumacher, J., Reich, P., Knops, J., Tilman, D., Craine, J., Ellsworth, D., Weigelt, A., Weisser, W., Buchmann, N., Scherer-Lorenzen, M., Kirwan, L., Luescher, A., Sebastia, M., Finn, J., Collins, R., Isbell, F., Wilsey, B., Yachi, S., Loreau, M., Tilman, D., Reich, P., Knops, J., van Ruijven, J., Berendse, F., Eisenhauer, N., Milcu, A., Allan, E., Nitschke, N., Scherber, C., Pimm, S., Gunderson, L., Tilman, D., Pfisterer, A., Schmid, B., van Ruijven, J., Berendse, F., Joshi, J., Matthies, D., Schmid, B., Pfisterer, A., Diemer, M., Schmid, B., Scherber, C., Heimann, J., Kohler, G., Mitschunas, N., Weisser, W., Tilman, D., Downing, J., Kahmen, A., Perner, J., Buchmann, N., Wang, Y., Yu, S., Wang, J., Leps, J., Osbornovakosinova, J., Rejmanek, M., Macgillivray, C., Grime, J., Band, S., Booth, R., Campbell, B., Gilgen, A., Buchmann, N., Grime, J., Brown, V., Thompson, K., Masters, G., Hillier, S., Hu, Z., Yu, G., Zhou, Y., Sun, X., Li, Y., Jentsch, A., Kreyling, J., Elmer, M., Gellesch, E., Glaser, B., Boeck, H.D., Lemmens, C., Bossuyt, H., Malchair, S., Carnol, M., Peer, L.V., Nijs, I., Reheul, D., Cauwer, B.D., Bessler, H., Temperton, V., Roscher, C., Buchmann, N., Schmid, B., Kreyling, J., Beierkuhnlein, C., Elmer, M., Pritsch, K., Radovski, M., Weisshuhn, K., Auge, H., Prati, D., Molyneux, D., Davies, W., Foulds, W., Roscher, C., Schumacher, J., Baade, J., Wilcke, W., Gleixner, G., Cop, J., Vidrih, M., Hacin, J., 2012. Grassland resistance and resilience after drought depends on management intensity and species richness. PLoS ONE 7, e36992. https://doi.org/10.1371/journal.pone.0036992.
Wingate, L., Ogée, J., Cremonese, E., Filippa, G., Mizunuma, T., Migliavacca, M., Moisy, C., Wilkinson, M., Moureaux, C., Wohlfahrt, G., Hammerle, A., Hoertnagl, L., Gimeno, C., Porcar-Castell, A., Galvagno, M., Nakaji, T., Morison, J., Kolle, O., Knohl, A., Kutsch, W., Kolari, P., Nikinmaa, E., Ibrom, A., Gielen, B., Eugster, W., Balzarolo, M., Papale, D., Klumpp, K., Koestner, B., Grunwald, T., Joffre, R., Ourcival, J.M., Hellstrom, M., Lindroth, A., George, C., Longdoz, B., Genty, B., Levula, J., Heinesch, B., Sprintsin, M., Yakir, D., Manise, T., Guyon, D., Ahrends, H., Plaza-Aguilar, A., Guan, J.H., Grace, J., 2015. Interpreting canopy development and physiology using a European phenology camera network at flux sites. Biogeosciences 12, 5995–6015. https://doi.org/10.5194/bg-12-5995-2015.
Wipf, S., Rixen, C., 2010. A review of snow manipulation experiments in Arctic and alpine tundra ecosystems. Polar Res. 29, 95–109. https://doi.org/10.1111/j.1751-8369.2010.00153.x http://www.polarresearch.net/index.php/polar/article/view/6054.
Wolf, S., Eugster, W., Ammann, C., Häni, M., Zielis, S., Hiller, R., Stieger, J., Imer, D., Merbold, L., Buchmann, N., 2013. Contrasting response of grassland versus forest carbon and water fluxes to spring drought in Switzerland. Environ. Res. Lett. 8, 035007. https://doi.org/10.1088/1748-9326/8/3/035007 http://stacks.iop.org/1748-9326/8/i=3/a=035007?key=crossref.c2748823ac9054a853ec0a4778f2bee7.

World Meteorological Organization, 2016. Statement on the Status of the Global Climate in 2015. Technical Report 1130.

Yang, X., Tang, J., Mustard, J., 2014. Comparing camera-based phenological metrics with leaf biochemical, biophysical, and spectral properties throughout the growing season of a temperate deciduous. J. Geophys. Res. 1–11. https://doi.org/10.1002/2013JG002460.

Zelikova, T.J., Williams, D.G., Hoenigman, R., Blumenthal, D.M., Morgan, J.A., Pendall, E., 2015. Seasonality of soil moisture mediates responses of ecosystem phenology to elevated CO_2 and warming in a semi-arid grassland. J. Ecol. https://doi.org/10.1111/1365-2745.12440.

Zhou, Y., Xiao, X., Wagle, P., Bajgain, R., Mahan, H., Basara, J.B., Dong, J., Qin, Y., Zhang, G., Luo, Y., Gowda, P.H., Neel, J.P., Starks, P.J., Steiner, J.L., 2017. Examining the short-term impacts of diverse management practices on plant phenology and carbon fluxes of Old World bluestems pasture. Agric. For. Meteorol. 237–238, 60–70. https://doi.org/10.1016/j.agrformet.2017.01.018 http://linkinghub.elsevier.com/retrieve/pii/S016819231730028X.

Zohner, C.M., Benito, B.M., Svenning, J.C., Renner, S.S., 2016. Day length unlikely to constrain climate-driven shifts in leaf-out times of northern woody plants. Nat. Clim. Change 6, https://doi.org/10.1038/nclimate3138.